IUEP-HEP-20-01

Measuring the trilinear Higgs boson self–coupling at the 100 TeV hadron collider via multivariate analysis

Jubin Park[1,2], Jung Chang[2], Kingman Cheung[3,4,5], and Jae Sik Lee[2,1]

[1] *IUEP, Chonnam National University, Gwangju 61186, Korea*

[2] *Department of Physics, Chonnam National University, Gwangju 61186, Korea*

[3] *Physics Division, National Center for Theoretical Sciences, Hsinchu, Taiwan*

[4] *Division of Quantum Phases and Devices, School of Physics, Konkuk University, Seoul 143-701, Republic of Korea*

[5] *Department of Physics, National Tsing Hua University, Hsinchu 300, Taiwan*

(Dated: September 11, 2020)

arXiv:2003.12281v2 [hep-ph] 11 Sep 2020

Abstract

We perform a multivariate analysis of Higgs-pair production via the decay channel $HH \to b\bar{b}\gamma\gamma$ at the future 100 TeV pp collider to determine the trilinear Higgs self–coupling (THSC) λ_{3H}, which takes the value of 1 in the standard model. We consider all known background processes. For the signal we adopt the most recent event generator of `POWHEG-BOX-V2` to exploit the NLO distributions for Toolkit for Multivariate Data Analysis (TMVA). Through the technique of Boosted Decision Tree (BDT) analysis trained for $\lambda_{3H} = 1$, compared to the the conventional cut-and-count approach, the signal-to-background ratio improves tremendously from about 1/10 to 1 and the significance can reach up to 20.5 with a luminosity of 3 ab^{-1} without including systematic uncertainties. In addition, by implementing a likelihood fitting of the signal-plus-background $M_{\gamma\gamma bb}$ distribution with optimized bin sizes, it is possible to determine the THSC with the precision of 7.5% at 68% CL even at the early stage of 100 TeV hadron collider with 3 ab^{-1}.

I. INTRODUCTION

Since the discovery of the 125 GeV Higgs boson in 2012 at the LHC [1], we have been looking for a clear signal or even a hint of new physics beyond the Standard Model (SM) but without much success. Moreover, after completing the Runs I and II at the LHC, it turns out that the 125 GeV Higgs boson is best described as the SM Higgs boson [2], although there is an upward trend in the overall signal strength [3]. Under this situation, one of the most solid avenues to explore for new physics is to measure the Higgs potential which could be significantly different from that of the SM.

Higgs-boson pair production at the high-luminosity and/or high-energy hadron colliders provides a very useful way to probe the Higgs potential via the investigation of the trilinear Higgs self-coupling (THSC) [4–6]. The specific decay modes considered are: $b\bar{b}b\bar{b}$ [7], $b\bar{b}\gamma\gamma$ [8, 9], $b\bar{b}\tau^+\tau^-$ [10], $b\bar{b}W^+W^-$ [11], and some combinations of these channels [12, 13]. Higgs-boson pair production also has been vastly studied in models beyond the SM [14].

The current limits on the THSC in units of λ_{3H}, which takes the value of 1 in the SM, are $-5.0 < \lambda_{3H} < 12$ from ATLAS [15] and $-11.8 < \lambda_{3H} < 18.8$ from CMS [16] at 95% confidence level (CL). At the high-luminosity option of the LHC running at 14 TeV (HL-LHC) with an integrated luminosity of 3 ab^{-1}, a combined ATLAS and CMS projection of the 68% CL interval is $0.57 < \lambda_{3H} < 1.5$ without including systematic uncertainties [17]. On the other hand, at the International Linear Collider (ILC) operated at 1 TeV can reach the precision of 10% at 68% CL with an integrated luminosity of 8 ab^{-1} [18, 19].

In this work, we perform a multivariate analysis of Higgs-pair production in $HH \to b\bar{b}\gamma\gamma$ channel at the 100 TeV hadron collider. In our previous work, based on the conventional cut-and-count analysis, it was shown that the THSC can be measured with about 20% accuracy at the SM value with a luminosity of 3 ab^{-1} [20]. In this Letter, with the use of the BDT method closely following Ref. [21], we show that the THSC can be measured with a precision of 7.5% at 68% CL at the 100 TeV hadron collider assuming 3 ab^{-1} luminosity, which is superior to the accuracy expected at the 1 TeV ILC even with 8 ab^{-1}.

II. EVENT GENERATION AND TMVA ANALYSIS

The Higgs bosons in the signal event samples are generated on-shell with a zero width by `POWHEG-BOX-V2` [22, 23] with the damping factor `hdamp` set to the default value of 250 to limit the amount of hard radiation. This code provides NLO distributions matched to a parton shower taking account of the full top-quark mass dependence. The signal cross section at NNLO order in QCD is calculated according to $\sigma^{\rm NNLO}(\lambda_{3H}) = K_{\rm SM}^{\rm NNLO/NLO}\,\sigma^{\rm NLO}(\lambda_{3H})$ using $\sigma^{\rm NLO}(\lambda_{3H})$ from `POWHEG-BOX-V2` and $K_{\rm SM}^{\rm NNLO/NLO} = 1.067$ [24] [1] in the FT approximation in which the full top-quark mass dependence is considered only in the real radiation while the Born improved Higgs Effective Field Theory is taken in the virtual part. And then, the `MadSpin` code [26] is used for the decay of both Higgs bosons into two bottom quarks and two photons.

For generation and simulation of backgrounds, we closely follow Ref. [20] [2], except for the use of the post-LHC PDF set of `CT14LO` [28] for non-resonant backgrounds. Furthermore, for the two main non-resonant backgrounds of $b\bar{b}\gamma\gamma$ and $c\bar{c}\gamma\gamma$, we use the merged cross sections and distributions by MLM matching [29, 30] with **xqcut** and $Q_{\rm cut}$ set to 20 GeV and 30 GeV, respectively. For the remaining non-resonant backgrounds, we are using the cross sections and distributions obtained by applying the generator-level cuts as adopted in Ref. [9, 13] which might provide more reliable and conservative estimation of the non-resonant backgrounds containing light jets [20].

For parton showering and hadronization, `PYTHIA8` [31] is used both for signal and backgrounds. Finally, fast-detector simulation and analysis are performed using `Delphes3` [32] with the `Delphes-FCC` template.

All the signal and backgrounds are summarized in Table I, together with information of the corresponding event generator, the cross section times the branching ratio and the order in QCD, and the Parton Distribution Function (PDF) used.

A multivariate analysis is performed using TMVA [34] with `ROOTv6.18` [35]. After applying a sequence of event selections as in Table II, we choose the following 8 kinematic

[1] According to the recent N3LO calculations [25], the signal cross section is further enhanced by the amount of 2.7% which would hardly affect our conclusion, or rather strengthen our results.

[2] Specifically, the multi-variate MV1 b-tagging algorithm with $\epsilon_b = 0.75$ is taken together with $P_{c\to b} = 0.1$, $P_{j\to b} = 0.01$, and $P_{j\to\gamma} = 1.35 \times 10^{-3}$ [27].

TABLE I. Monte Carlo samples used in Higgs-pair production analysis $H(\to b\bar{b})H(\to \gamma\gamma)$, and the corresponding codes for the matrix-element generation. `PYTHIA8` is used for parton showering and hadronization. We refer to Ref. [33] for `MG5_aMC@NLO`.

Signal					
Signal process		Generator	$\sigma \cdot BR$ [fb]	Order in QCD	PDF used
$gg \to HH \to b\bar{b}\gamma\gamma$		`POWHEG-BOX-V2`	3.25	NNLO	PDF4LHC15_nlo
Backgrounds					
Background(BG)	Process	Generator	$\sigma \cdot BR$ [fb]	Order in QCD	PDF used
Single-Higgs associated BG	$ggH(\to \gamma\gamma)$	`POWHEG − BOX`	1.82×10^3	NNNLO	`CT10`
	$t\bar{t}H(\to \gamma\gamma)$	`PYTHIA8`	7.29×10^1	NLO	
	$ZH(\to \gamma\gamma)$	`PYTHIA8`	2.54×10^1	NNLO	
	$b\bar{b}H(\to \gamma\gamma)$	`PYTHIA8`	1.96×10^1	NNLO(5FS)	
Non-resonant BG	$b\bar{b}\gamma\gamma$	`MG5_aMC@NLO`	2.28×10^3	LO	CT14LO
	$c\bar{c}\gamma\gamma$	`MG5_aMC@NLO`	1.92×10^4	LO	MLM [29, 30]
	$jj\gamma\gamma$	`MG5_aMC@NLO`	4.20×10^5	LO	CT14LO Refs. [9, 13, 20]
	$b\bar{b}j\gamma$	`MG5_aMC@NLO`	0.96×10^7	LO	
	$c\bar{c}j\gamma$	`MG5_aMC@NLO`	3.19×10^7	LO	
	$b\bar{b}jj$	`MG5_aMC@NLO`	1.00×10^{10}	LO	
	$Z(\to b\bar{b})\gamma\gamma$	`MG5_aMC@NLO`	7.87×10^1)	LO	
$t\bar{t}$ and $t\bar{t}\gamma$ BG (≥ 1 lepton)	$t\bar{t}$	`MG5_aMC@NLO`	1.76×10^7	NLO	`CT10`
	$t\bar{t}\gamma$	`MG5_aMC@NLO`	4.18×10^4	NLO	`CTEQ6L1`

variables for TMVA:

$$M_{bb}\,,\quad P_T^{bb}\,,\quad \Delta R_{bb}\,;\quad M_{\gamma\gamma}\,,\quad P_T^{\gamma\gamma}\,,\quad \Delta R_{\gamma\gamma}\,;\quad M_{\gamma\gamma bb}\,,\quad \Delta R_{\gamma b}\,.$$

The judicious choice of the two photons or two b quarks for the above TMVA variables has been made as in [21]. We also refer to Ref. [21] for the details of our TMVA setup and analysis. And we choose BDT for our analysis since the BDT-related methods show higher performance with better signal efficiency and stronger background rejection.

TABLE II. Sequence of event selection criteria applied in this analysis.

Sequence	Event Selection Criteria at the 100 TeV hadron collider
1	Di-photon trigger condition, ≥ 2 isolated photons with $P_T > 30$ GeV, $\|\eta\| < 5$
2	≥ 2 isolated photons with $P_T > 40$ GeV, $\|\eta\| < 3$, $\Delta R_{j\gamma,\gamma\gamma} > 0.4$
3	≥ 2 jets identified as b-jets with leading(subleading) $P_T > 50(40)$ GeV, $\|\eta\| < 3$, $\Delta R_{bb} > 0.4$
4	Events are required to contain ≤ 5 jets with $P_T > 40$ GeV within $\|\eta\| < 5$
5	No isolated leptons with $P_T > 40$ GeV, $\|\eta\| < 3$
6	TMVA analysis

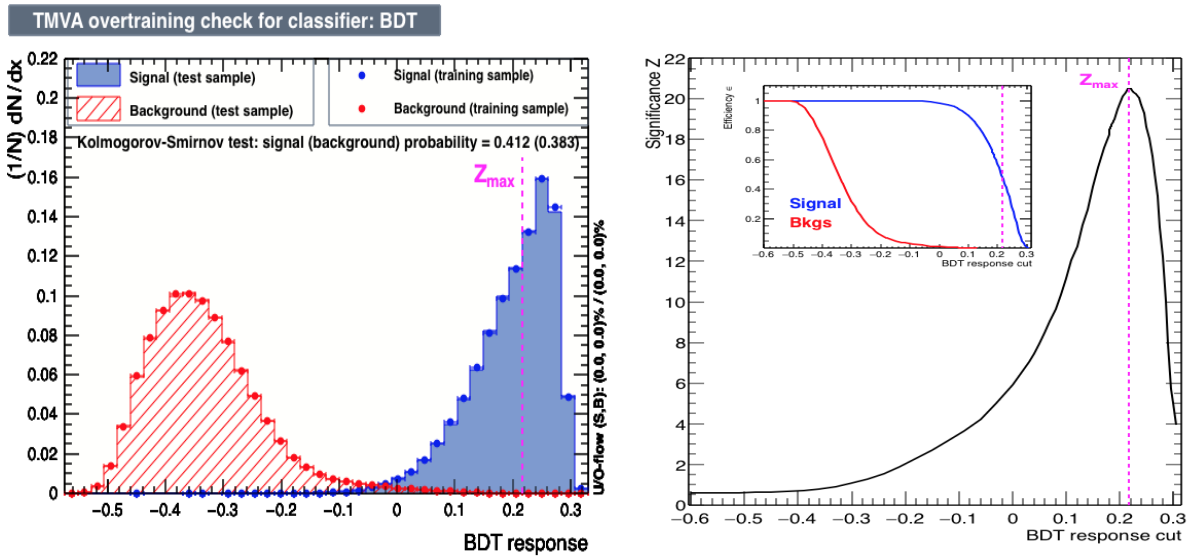


FIG. 1. (Left) Normalized SM BDT responses for test (histogram) and training (dots with error bars) samples. BDT responses for signal (blue) and background (red) samples, which mostly populate in the regions with positive and negative BDT response, respectively. (Right) Signal and background efficiencies (inset) and significance Z as functions of BDT response cut. BDT_{SM} is used. The vertical lines show the position of the optimal cut on the BDT response which maximizes the significance.

III. RESULTS

In the left panel of Fig. 1, we show the BDT responses obtained using BDT trained for $\lambda_{3H} = 1$ which is dubbed as BDT_{SM}. By validating the BDT distributions for the training sample (dots with error bars) with those for the test sample (histogram),

we check that $\mathrm{BDT_{SM}}$ is not overtrained. In the right panel of Fig. 1, using $\mathrm{BDT_{SM}}$, we show the behavior of signal and background efficiencies (inset) and significance $Z = \sqrt{2 \cdot [((s+b) \cdot \ln(1+s/b) - s)]}$ with s and b being the numbers of signal and background events as functions of the cut value on BDT response. The significance can reach up to 20.50 when the BDT response is cut at 0.216, at which, the signal and background efficiencies are 0.48 and 1.58×10^{-4}, respectively. We denote by vertical lines the positions of the optimal cut on the BDT response which maximizes the significance.

In Table III, we present the expected number of signal and background events at the 100 TeV hadron collider assuming 3 $\mathrm{ab^{-1}}$ using $\mathrm{BDT_{SM}}$ with the BDT response cut of 0.216. We show the four representative values of λ_{3H} for signal and the backgrounds are separated into three categories. For comparisons, we also show the results obtained using the cut-and-count analysis [20]. In the last column, we additionally present the effective luminosity (Eff. Lumi.) for each of signal and background samples. In the $t\bar{t}$ and $t\bar{t}\gamma$ backgrounds, the first (second) number is the effective luminosity when the two top quarks decay fully (semi-) leptonically. We find about 550 signal and 550 background events for $\lambda_{3H} = 1$. Comparing to the results using the cut-and-count analysis [20], the number of signal events decreases by only 19% while the number of backgrounds by almost 90%, resulting in an increase in significance from 8.44 to 20.50. Note that the composition of backgrounds changes drastically by the use of BDT. In the cut-and-count analysis, the non-resonant background is about two times larger than the single-Higgs associated background. While, in the BDT analysis, the single-Higgs associated background is more than four times larger than the non-resonant one and $t\bar{t}$ associated background becomes negligible. Note that we generate relatively smaller number of events for the $c\bar{c}\gamma\gamma$, $c\bar{c}j\gamma$, and $b\bar{b}jj$ backgrounds since we observe that they quickly decrease when the BDT response cut approaches to the point $Z_{\max}$ of 0.216 [3]. Specifically, the $b\bar{b}jj$ background vanishes for the BDT response cut larger than 0.2. Otherwise, we generate enough number of events considering the assumed luminosity of 3 $\mathrm{ab^{-1}}$.

First, we try to determine the THSC considering the total number of events. As shown in the left panel of Fig. 2, we find that the THSC can be measured with about 11% accuracy at the SM value which is about two times better than the result based on the conventional cut-and-count analysis [20]. However, there is a second solution around $\lambda_{3H} = 6.5$. To lift

[3] In fact, there are some differences in kinematic distributions among the non-resonant backgrounds. For example, the $c\bar{c}\gamma\gamma$ background is more populated in the region of $\Delta R_{bb} > 3$ compared to the $b\bar{b}\gamma\gamma$ one.

TABLE III. Expected number of signal and background events at the 100 TeV hadron collider assuming 3 ab^{-1} using BDT$_{\rm SM}$ with the BDT response cut of 0.216. See text for explanation.

	Expected yields (3 ab^{-1})			
Signal and Backgrounds	Pre-Selection	BDT$_{\rm SM}$	Cut-and -Count	Eff. Lumi. (ab^{-1})
$H(b\bar{b})\,H(\gamma\gamma)$, $\lambda_{3H}=-3$	7253.98	2408.37	3400.08	10.7
$H(b\bar{b})\,H(\gamma\gamma)$, $\lambda_{3H}=0$	2072.09	902.49	1146.21	44.5
$\mathbf{H(b\bar{b})\,H(\gamma\gamma)}$, $\boldsymbol{\lambda_{3H}=1}$	**1124.48**	**548.02**	**673.29**	**615**
$H(b\bar{b})\,H(\gamma\gamma)$, $\lambda_{3H}=5$	1480.24	251.13	439.29	40.9
$gg\,H(\gamma\gamma)$	5827.41	255.86	875.71	17.0
$t\bar{t}\,H(\gamma\gamma)$	11371.21	145.88	868.73	13.2
$Z\,H(\gamma\gamma)$	593.29	38.88	168.86	39.4
$b\bar{b}\,H(\gamma\gamma)$	205.45	2.59	9.82	51.0
$b\bar{b}\,\gamma\gamma$	183493.56	55.01	336.49	19.2
$c\bar{c}\,\gamma\gamma$	66600.78	0.00	54.66	0.11
$j\,j\,\gamma\gamma$	14182.56	2.52	25.20	2.38
$b\bar{b}\,j\,\gamma$	1228956.91	38.53	1176.93	3.74
$c\bar{c}\,j\,\gamma$	208285.83	0.00	187.92	0.26
$b\bar{b}\,j\,j$	1622778.23	0.00	2231.08	0.19
$Z(b\bar{b})\,\gamma\gamma$	4540.20	4.72	45.33	12.7
$t\bar{t}$ (≥ 1 leptons)	78490.03	0.00	56.93	$11.5+3.68$
$t\bar{t}\,\gamma$ (≥ 1 leptons)	74885.54	9.09	105.16	$8.69+2.07$
Total Background	3500211.00	553.09	6142.83	
Significance Z, $\lambda_{3H}=1$		**20.50**	**8.44**	

up the two-fold ambiguity, we implement a likelihood fitting of the signal-plus-background $M_{\gamma\gamma bb}$ distribution and find the second solution is ruled out by more than 8σ confidence, see the right panel of Fig. 2.

To improve the sensitivity of the THSC around the SM value and to tame the statistical

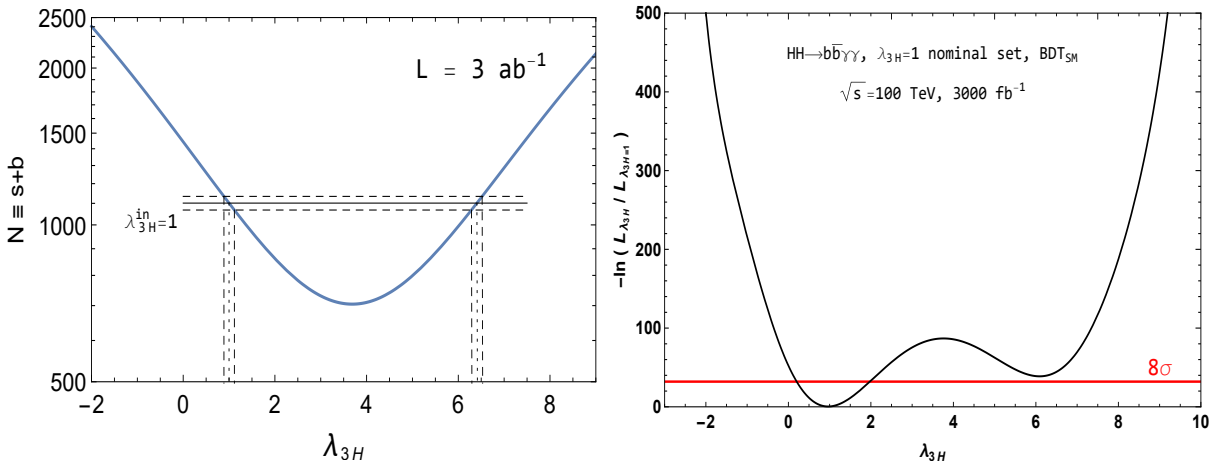


FIG. 2. (Left) The total number $N = s+b$ of signal (s) and background (b) events versus λ_{3H} with 3 ab^{-1}. The horizontal solid line denotes the total number of events obtained using the SM value of $\lambda_{3H} = 1$ and the dashed lines for the statistical 1-σ error. (Right) The relative log likelihood distribution for the nominal value of $\lambda_{3H} = 1$ at the 100 TeV hadron collider assuming 3 ab^{-1} and using BDT$_{\rm SM}$ with the BDT response cut of 0.216. The distribution has been obtained by a likelihood fitting of $M_{\gamma\gamma bb}$ distribution for each value of λ_{3H}. The black solid line shows the result of a polynomial fitting and the horizontal solid (red) line at $-\ln(L_{\lambda_{3H}}/L_{\lambda_{3H}=1}) = 32$ indicates the value corresponding to the 8σ level.

fluctuation due to the limited size of the MC samples, we repeat the likelihood fitting of $M_{\gamma\gamma bb}$ distribution by optimizing the bin size between 1/20 GeV and 1/60 GeV. Finally, we find that the THSC can be determined with a precision of 7.5% at 68% CL as shown in the left panel of Fig. 3. In the right panel of Fig. 3, $M_{\gamma\gamma bb}$ distributions are shown for the THSC at the SM value and for the two values deviated by 1σ.

By now, we have considered only the statistical uncertainties which may eventually dominate the total uncertainties. Before concluding, we would like to discuss the effects of systematic uncertainties which could be important at the early stage of 100 TeV hadron collider. The systematic uncertainties might be taken into account by considering the variance of background σ_b^2 [36]. In this case, the error due to systematic uncertainties is proportional to the number of background or $\sigma_b \propto b$. We find that the THSC precision of 7.5%−18% at 68% CL while varying σ_b/b between 0 and 0.2, see Fig. 4 [4].

Finally, before we end this section, in Table IV, we show the relative importance of the

[4] Incidentally, by measuring only the total number of events, the precision becomes worse to 11%−30%.

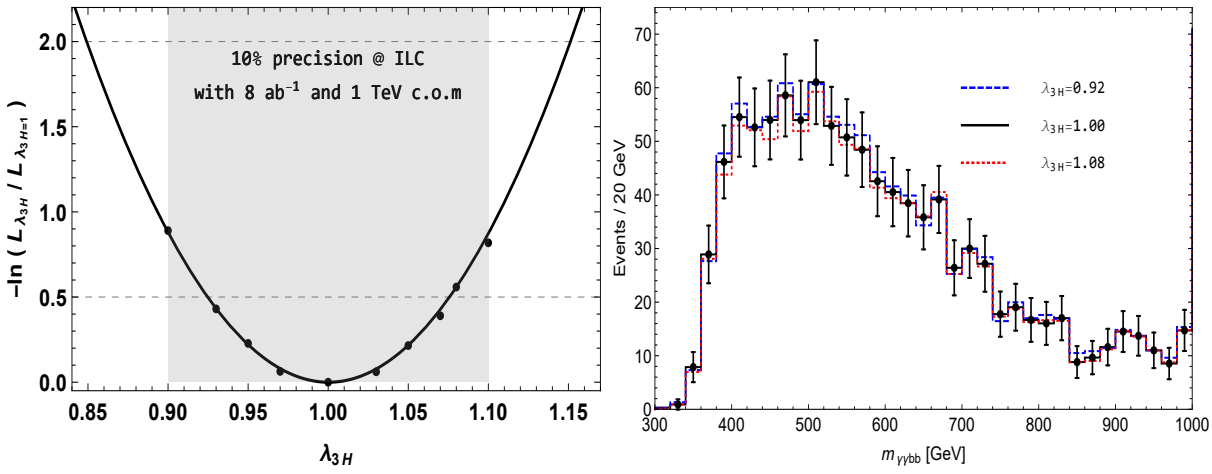


FIG. 3. (Left) The relative log likelihood distribution for the nominal value of $\lambda_{3H} = 1$ at the 100 TeV hadron collider with 3 ab^{-1}. The black circles are the values obtained by a likelihood fitting of $M_{\gamma\gamma bb}$ distributions using BDT$_{\rm SM}$ with the BDT response cut of 0.216. The black solid line shows the result of a polynomial fitting and the thin dashed line at 0.5 (2.0) indicates the value corresponding to a 1σ (2σ) CI. The shaded region shows the 1σ CI expected at the ILC at 1 TeV with 8 ab^{-1}. (Right) The SM $M_{\gamma\gamma bb}$ distribution (solid line with dots with 1σ error bars) and those for $\lambda_{3H} = 0.92$ and 1.08 (dashed lines).

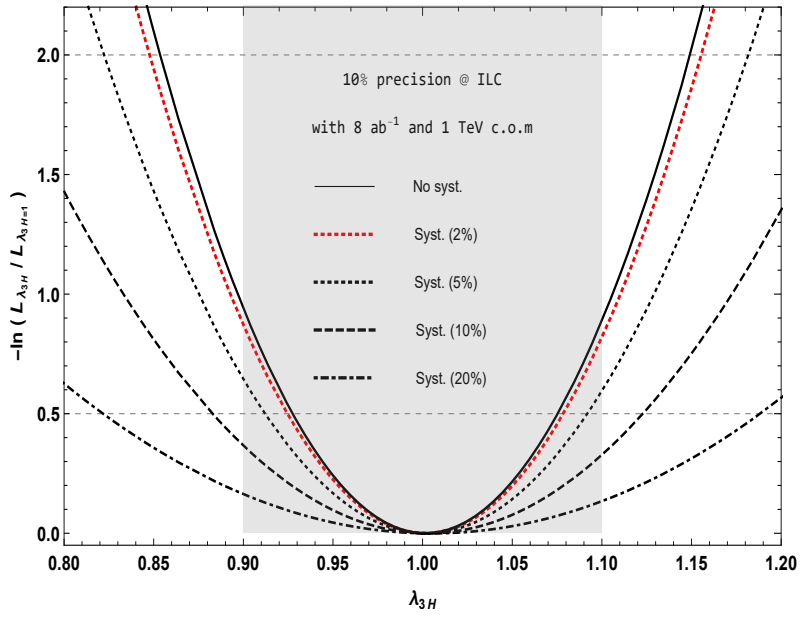


FIG. 4. The same as in the left panel of Fig. 3 while taking $\sigma_b/b = 0$ (solid), 0.02 (red dotted) 0.05 (black dotted), 0.1 (dashed), and 0.2 (dash-dotted).

variables that we employed in this BDT analysis. We observe that the two most important variables are ΔR_{bb} and $\Delta R_{\gamma\gamma}$, which is consistent with our previous cut-and-count analysis [20].

TABLE IV. The ranking of the variables that we employed in this BDT analysis in the descending order of importance.

ΔR_{bb}	$\Delta R_{\gamma\gamma}$	$M_{\gamma\gamma}$	$\Delta R_{\gamma b}$	$P_T^{\gamma\gamma}$	$M_{\gamma\gamma bb}$	P_T^{bb}	M_{bb}
0.163	0.152	0.150	0.133	0.110	0.102	0.096	0.095

IV. CONCLUSIONS:

Higgs-pair production is one of the most useful avenue to probe the EWSB sector. We have studied in great details, with the help of machine learning, the sensitivity of measuring the THSC λ_{3H} that one can expect at the 100 TeV pp collider with an integrated luminosity 3 ab^{-1}. With TMVA one can improve the signal-to-background ratio for $\lambda_{3H} = 1$ to 1 : 1 compared with the ratio 1 : 10 obtained in the conventional cut-and-count approach. Furthermore, the significance of such a signal jumps to 20.

Other than determining the THSC by measuring the total number of events, one can also improve the sensitivity and lift the two-fold degeneracy by implementing a likelihood fitting of the signal-plus-background $M_{\gamma\gamma bb}$ distribution with optimized bin sizes. The THSC can be determined with a precision of 7.5% at 68% CL with 3 ab^{-1}, which is indeed better than the ILC running at 1 TeV with 8 ab^{-1}. Extrapolating our result conservatively, we expect that one can achieve the precision better than $\sim 2\%$ with 30 ab^{-1}.

Note added: After the completion of our work, we learned a similar analysis performed considering various systematic uncertainties rigorously [37]. They found the combined precision of 2.9%−5.5% with 30 ab^{-1} at 68% CL which is in a good quantitative agreement with our results.

APPENDIX

Appendix A: More on the $c\bar{c}\gamma\gamma$, $c\bar{c}j\gamma$, and $b\bar{b}jj$ backgrounds

For this work, we generate relatively smaller number of events for the $c\bar{c}\gamma\gamma$, $c\bar{c}j\gamma$, and $b\bar{b}jj$ backgrounds which may lead to underestimation of the relevant backgrounds.

The $c\bar{c}\gamma\gamma$ and $c\bar{c}j\gamma$ backgrounds might be negligible since, taking account of the fake rates $P_{c\to b}$ and $P_{j\to\gamma}$, the cross sections are smaller than that of the $b\bar{b}\gamma\gamma$ background by about an order of magnitude. On the other hand, our estimation of the $b\bar{b}jj$ background could be unreliable due to the limited size of the MC sample. Here we try to estimate the background yield based on the current sample.

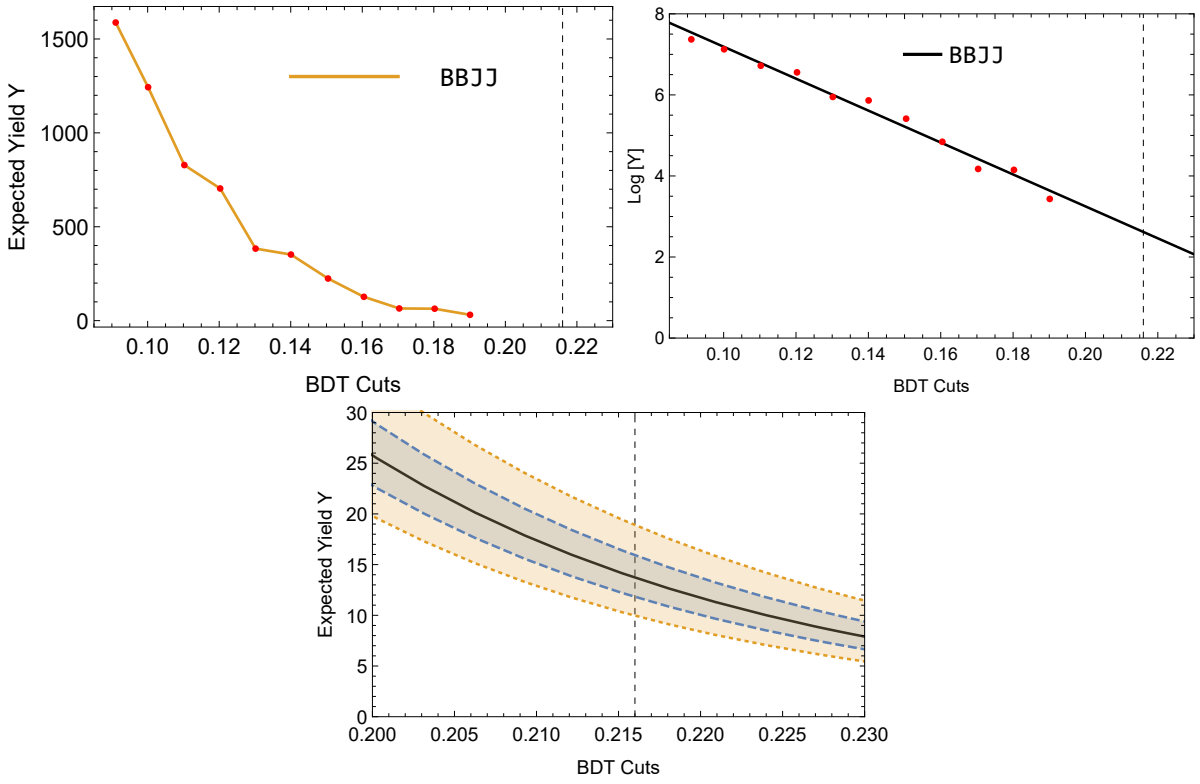


FIG. 5. Behavior of the $b\bar{b}jj$ background yield $Y_{b\bar{b}jj}$ versus the BDT response cut. In the upper panels, the MC data points are denoted by bullets and the solid line in the upper-right panel shows the result of the linear fitting to $\log Y_{b\bar{b}jj}$. In the lower panel, we show the result of extrapolation of the solid line to the region with BDT Cut > 0.19, where no data points exist, together with 1- and 2-σ errors. The vertical lines locate the BDT response cut of 0.216 taken for $\mathrm{BDT_{SM}}$.

Precisely, we study the behavior of the $b\bar{b}jj$ background yield $Y_{b\bar{b}jj}$ versus the BDT

response cut. First we observe that, based on the current $b\bar{b}jj$ MC sample, our estimation of the background results in 0 when BDT Cut > 0.19, see the upper-left panel of Fig. 5. To extrapolate to the region with BDT Cut > 0.19, we implement a linear fitting to $\log Y_{b\bar{b}jj}$, see the solid line in the upper-right panel of Fig. 5. And we find that

$$Y_{b\bar{b}jj} = 13.7^{+2.2\,(5.2)}_{-1.9\,(3.7)} \tag{A.1}$$

at 68(95)% CL as shown in the lower panel of Fig. 5. Taking the 1σ upper value of 15.9, the number of total background increases by the amount of about 3% which hardly affect our main results significantly.

Incidentally, we note that the $jj\gamma\gamma$ background survives though its cross section is smaller than that of the $b\bar{b}\gamma\gamma$ one by about *two* orders of magnitude taking account of the fake rate $P_{j\to b}$. This is because its kinematical distributions quite resemble to those of the signal. For example, compared to other non-resonant backgrounds, we find that it is quite populated in the region of $\Delta R_{bb} \lesssim 2$ where most signal events are located.

Appendix B: Supplemental materials

In this appendix, we present the normalized distributions of the eight kinematic variables for the SM signal with $\lambda_{3H} = 1$ (black solid) and the six non-resonant backgrounds after applying the event preselection cuts 1-5 in Table II, see Fig. 6. For $M_{bb\,,\gamma\gamma}$ and $P_T^{bb\,,\gamma\gamma}$, in terms of P_T, we choose the least energetic two photons or two b quarks while the most energetic ones are chosen for $\Delta R_{bb,\gamma\gamma}$ and $M_{\gamma\gamma bb}$. For $\Delta R_{\gamma b}$, on the other hand, we choose the least energetic b and the next-to-the-least energetic photon.

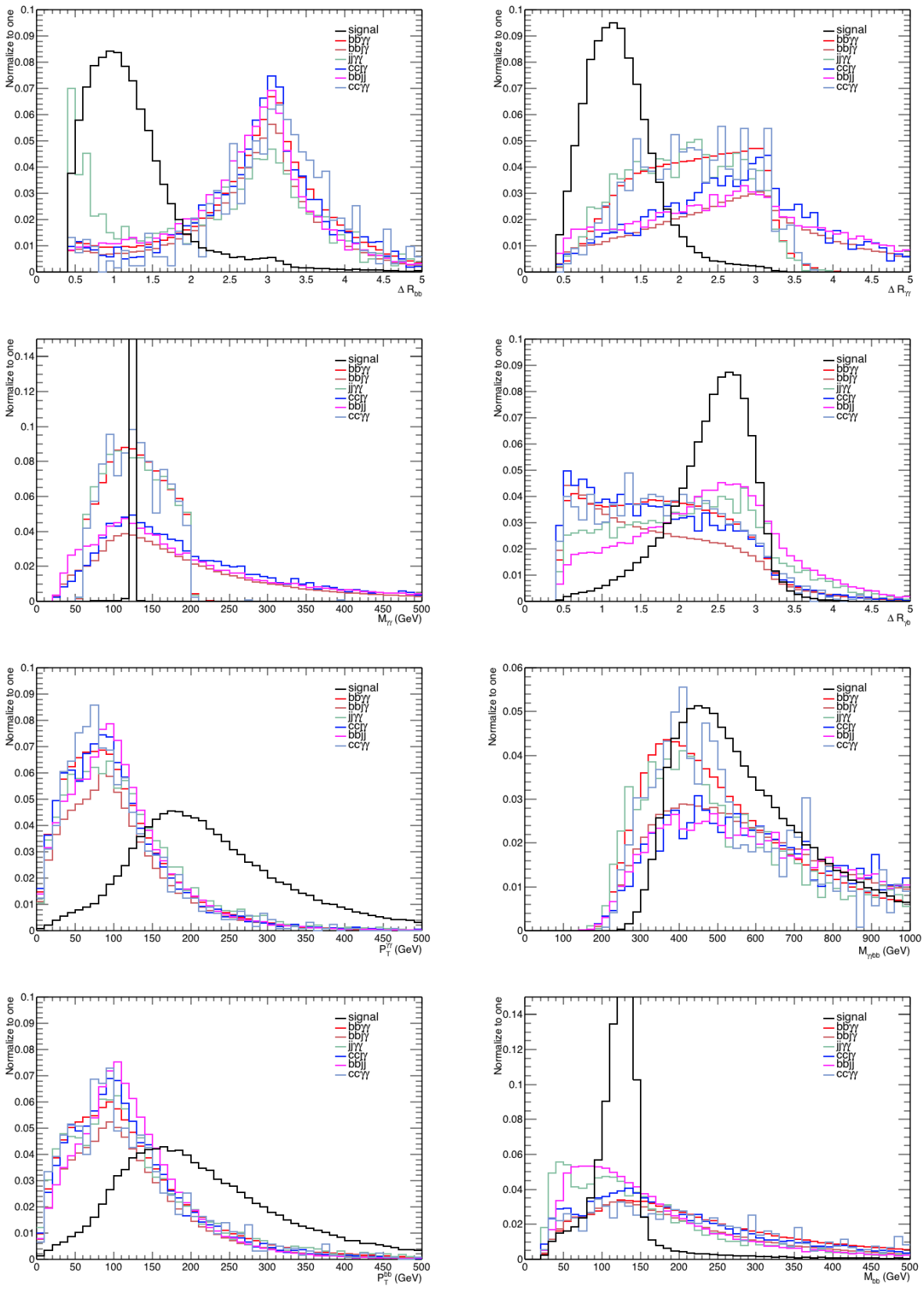


FIG. 6. Normalized distributions of the eight kinematic variables for the SM signal and six non-resonant backgrounds after applying the event preselection cuts 1-5 in Table II. Panels are in the descending order of importance (see Table IV) from upper-left to lower-right.

ACKNOWLEDGMENT

This work was supported by the National Research Foundation of Korea Grant No. NRF-2016R1E1A1A01943297 (J.C., J.S.L., J.P.), No. NRF-2018R1D1A1B07051126 (J. P.), and by the MoST of Taiwan under Grant No. 107-2112-M-007-029-MY3 (K. C.).

---

[1] G. Aad *et al.* [ATLAS Collaboration], "Observation of a new particle in the search for the Standard Model Higgs boson with the ATLAS detector at the LHC," Phys. Lett. B **716**, 1 (2012) [arXiv:1207.7214 [hep-ex]];
S. Chatrchyan *et al.* [CMS Collaboration], "Observation of a new boson at a mass of 125 GeV with the CMS experiment at the LHC," Phys. Lett. B **716**, 30 (2012) [arXiv:1207.7235 [hep-ex]].

[2] K. Cheung, J. S. Lee and P. Y. Tseng, "Higgs Precision (Higgcision) Era begins," JHEP **1305** (2013) 134 doi:10.1007/JHEP05(2013)134 [arXiv:1302.3794 [hep-ph]];
K. Cheung, J. S. Lee and P. Y. Tseng, "Higgs precision analysis updates 2014," Phys. Rev. D **90** (2014) 095009 doi:10.1103/PhysRevD.90.095009 [arXiv:1407.8236 [hep-ph]];

[3] K. Cheung, J. S. Lee and P. Y. Tseng, "New Emerging Results in Higgs Precision Analysis Updates 2018 after Establishment of Third-Generation Yukawa Couplings," JHEP **1909**, 098 (2019) doi:10.1007/JHEP09(2019)098 [arXiv:1810.02521 [hep-ph]].

[4] E. W. N. Glover and J. J. van der Bij, "Higgs Boson Pair Production Via Gluon Fusion," Nucl. Phys. B **309** (1988) 282. doi:10.1016/0550-3213(88)90083-1
D. A. Dicus, C. Kao and S. S. D. Willenbrock, "Higgs Boson Pair Production From Gluon Fusion," Phys. Lett. B **203** (1988) 457. doi:10.1016/0370-2693(88)90202-X
T. Plehn, M. Spira and P. M. Zerwas, "Pair production of neutral Higgs particles in gluon-gluon collisions," Nucl. Phys. B **479** (1996) 46 Erratum: [Nucl. Phys. B **531** (1998) 655] doi:10.1016/0550-3213(96)00418-X, 10.1016/S0550-3213(98)00406-4 [hep-ph/9603205].
A. Djouadi, W. Kilian, M. Muhlleitner and P. M. Zerwas, "Production of neutral Higgs boson pairs at LHC," Eur. Phys. J. C **10** (1999) 45 doi:10.1007/s100529900083 [hep-ph/9904287].
S. Dawson, S. Dittmaier and M. Spira, "Neutral Higgs boson pair production at hadron colliders: QCD corrections," Phys. Rev. D **58** (1998) 115012 doi:10.1103/PhysRevD.58.115012

[hep-ph/9805244].

U. Baur, T. Plehn and D. L. Rainwater, "Determining the Higgs boson selfcoupling at hadron colliders," Phys. Rev. D **67** (2003) 033003 doi:10.1103/PhysRevD.67.033003 [hep-ph/0211224]; T. Binoth, S. Karg, N. Kauer and R. Ruckl, "Multi-Higgs boson production in the Standard Model and beyond," Phys. Rev. D **74** (2006) 113008 doi:10.1103/PhysRevD.74.113008 [hep-ph/0608057].

[5] J. Baglio, A. Djouadi, R. Grber, M. M. Mhlleitner, J. Quevillon and M. Spira, "The measurement of the Higgs self-coupling at the LHC: theoretical status," JHEP **1304**, 151 (2013) doi:10.1007/JHEP04(2013)151 [arXiv:1212.5581 [hep-ph]].

J. Cao, Z. Heng, L. Shang, P. Wan and J. M. Yang, "Pair Production of a 125 GeV Higgs Boson in MSSM and NMSSM at the LHC," JHEP **1304** (2013) 134 doi:10.1007/JHEP04(2013)134 [arXiv:1301.6437 [hep-ph]].

D. de Florian and J. Mazzitelli, "Two-loop virtual corrections to Higgs pair production," Phys. Lett. B **724** (2013) 306 doi:10.1016/j.physletb.2013.06.046 [arXiv:1305.5206 [hep-ph]].

J. Grigo, J. Hoff, K. Melnikov and M. Steinhauser, "On the Higgs boson pair production at the LHC," Nucl. Phys. B **875** (2013) 1 doi:10.1016/j.nuclphysb.2013.06.024 [arXiv:1305.7340 [hep-ph]].

D. T. Nhung, M. Muhlleitner, J. Streicher and K. Walz, "Higher Order Corrections to the Trilinear Higgs Self-Couplings in the Real NMSSM," JHEP **1311** (2013) 181 doi:10.1007/JHEP11(2013)181 [arXiv:1306.3926 [hep-ph]].

U. Ellwanger, "Higgs pair production in the NMSSM at the LHC," JHEP **1308** (2013) 077 doi:10.1007/JHEP08(2013)077 [arXiv:1306.5541 [hep-ph]].

[6] E. Asakawa, D. Harada, S. Kanemura, Y. Okada and K. Tsumura, "Higgs boson pair production in new physics models at hadron, lepton, and photon colliders," Phys. Rev. D **82** (2010) 115002 doi:10.1103/PhysRevD.82.115002 [arXiv:1009.4670 [hep-ph]].

R. Contino, M. Ghezzi, M. Moretti, G. Panico, F. Piccinini and A. Wulzer, "Anomalous Couplings in Double Higgs Production," JHEP **1208** (2012) 154 doi:10.1007/JHEP08(2012)154 [arXiv:1205.5444 [hep-ph]].

G. D. Kribs and A. Martin, "Enhanced di-Higgs Production through Light Colored Scalars," Phys. Rev. D **86** (2012) 095023 doi:10.1103/PhysRevD.86.095023 [arXiv:1207.4496 [hep-ph]].

S. Dawson, E. Furlan and I. Lewis, "Unravelling an extended quark sector through multiple Higgs production?," Phys. Rev. D **87** (2013) no.1, 014007 doi:10.1103/PhysRevD.87.014007 [arXiv:1210.6663 [hep-ph]].

M. J. Dolan, C. Englert and M. Spannowsky, "New Physics in LHC Higgs boson pair production," Phys. Rev. D **87** (2013) no.5, 055002 doi:10.1103/PhysRevD.87.055002 [arXiv:1210.8166 [hep-ph]].

M. Gouzevitch, A. Oliveira, J. Rojo, R. Rosenfeld, G. P. Salam and V. Sanz, "Scale-invariant resonance tagging in multijet events and new physics in Higgs pair production," JHEP **1307** (2013) 148 doi:10.1007/JHEP07(2013)148 [arXiv:1303.6636 [hep-ph]].

R. S. Gupta, H. Rzehak and J. D. Wells, "How well do we need to measure the Higgs boson mass and self-coupling?," Phys. Rev. D **88** (2013) 055024 doi:10.1103/PhysRevD.88.055024 [arXiv:1305.6397 [hep-ph]].

[7] U. Baur, T. Plehn and D. L. Rainwater, "Examining the Higgs boson potential at lepton and hadron colliders: A Comparative analysis," Phys. Rev. D **68** (2003) 033001 doi:10.1103/PhysRevD.68.033001 [hep-ph/0304015].

D. E. Ferreira de Lima, A. Papaefstathiou and M. Spannowsky, "Standard model Higgs boson pair production in the ($b\bar{b}$)($b\bar{b}$) final state," JHEP **1408** (2014) 030 doi:10.1007/JHEP08(2014)030 [arXiv:1404.7139 [hep-ph]].

C. Englert, F. Krauss, M. Spannowsky and J. Thompson, "Di-Higgs phenomenology in $t\bar{t}hh$: The forgotten channel," Phys. Lett. B **743** (2015) 93 doi:10.1016/j.physletb.2015.02.041 [arXiv:1409.8074 [hep-ph]].

T. Liu and H. Zhang, "Measuring Di-Higgs Physics via the $t\bar{t}hh \to t\bar{t}b\bar{b}b\bar{b}$ Channel," arXiv:1410.1855 [hep-ph].

J. K. Behr, D. Bortoletto, J. A. Frost, N. P. Hartland, C. Issever and J. Rojo, "Boosting Higgs pair production in the $b\bar{b}b\bar{b}$ final state with multivariate techniques," Eur. Phys. J. C **76** (2016) no.7, 386 doi:10.1140/epjc/s10052-016-4215-5 [arXiv:1512.08928 [hep-ph]].

F. Bishara, R. Contino and J. Rojo, "Higgs pair production in vector-boson fusion at the LHC and beyond," Eur. Phys. J. C **77**, no. 7, 481 (2017) doi:10.1140/epjc/s10052-017-5037-9 [arXiv:1611.03860 [hep-ph]].

[8] U. Baur, T. Plehn and D. L. Rainwater, "Measuring the Higgs boson self coupling at the LHC and finite top mass matrix elements," Phys. Rev. Lett. **89** (2002) 151801

doi:10.1103/PhysRevLett.89.151801 [hep-ph/0206024];

U. Baur, T. Plehn and D. L. Rainwater, "Probing the Higgs selfcoupling at hadron colliders using rare decays," Phys. Rev. D **69** (2004) 053004 doi:10.1103/PhysRevD.69.053004 [hep-ph/0310056];

V. Barger, L. L. Everett, C. B. Jackson and G. Shaughnessy, "Higgs-Pair Production and Measurement of the Triscalar Coupling at LHC(8,14)," Phys. Lett. B **728** (2014) 433 doi:10.1016/j.physletb.2013.12.013 [arXiv:1311.2931 [hep-ph]];

W. Yao, "Studies of measuring Higgs self-coupling with $HH \to b\bar{b}\gamma\gamma$ at the future hadron colliders," arXiv:1308.6302 [hep-ph].

ATLAS collaboration, "Prospects for measuring Higgs pair production in the channel $H(\to \gamma\gamma)H(\to b\bar{b})$ using the ATLAS detector at the HL-LHC," ATL-PHYS-PUB-2014-019.

A. J. Barr, M. J. Dolan, C. Englert, D. E. Ferreira de Lima and M. Spannowsky, "Higgs Self-Coupling Measurements at a 100 TeV Hadron Collider," JHEP **1502** (2015) 016 doi:10.1007/JHEP02(2015)016 [arXiv:1412.7154 [hep-ph]].

A. Azatov, R. Contino, G. Panico and M. Son, "Effective field theory analysis of double Higgs boson production via gluon fusion," Phys. Rev. D **92** (2015) no.3, 035001 doi:10.1103/PhysRevD.92.035001 [arXiv:1502.00539 [hep-ph]].

A. Alves, T. Ghosh and K. Sinha, "Can We Discover Double Higgs Production at the LHC?," Phys. Rev. D **96** (2017) no.3, 035022 doi:10.1103/PhysRevD.96.035022 [arXiv:1704.07395 [hep-ph]].

D. Gonalves, T. Han, F. Kling, T. Plehn and M. Takeuchi, "Higgs boson pair production at future hadron colliders: From kinematics to dynamics," Phys. Rev. D **97**, no. 11, 113004 (2018) doi:10.1103/PhysRevD.97.113004 [arXiv:1802.04319 [hep-ph]].

S. Homiller and P. Meade, "Measurement of the Triple Higgs Coupling at a HE-LHC," JHEP **1903**, 055 (2019) doi:10.1007/JHEP03(2019)055 [arXiv:1811.02572 [hep-ph]].

[9] ATLAS Collaboration, "Study of the double Higgs production channel H(→ bb)H(→gamma gamma) with the ATLAS experiment at the HL-LHC," ATL-PHYS-PUB-2017-001, 2017, url: http://cds.cern.ch/record/2243387.

[10] A. J. Barr, M. J. Dolan, C. Englert and M. Spannowsky, "Di-Higgs final states augMT2ed – selecting hh events at the high luminosity LHC," Phys. Lett. B **728** (2014) 308 doi:10.1016/j.physletb.2013.12.011 [arXiv:1309.6318 [hep-ph]].

M. J. Dolan, C. Englert, N. Greiner and M. Spannowsky, "Further on up the road: $hhjj$ production at the LHC," Phys. Rev. Lett. **112** (2014) 101802 doi:10.1103/PhysRevLett.112.101802 [arXiv:1310.1084 [hep-ph]].

[11] A. Papaefstathiou, L. L. Yang and J. Zurita, "Higgs boson pair production at the LHC in the $b\bar{b}W^+W^-$ channel," Phys. Rev. D **87** (2013) no.1, 011301 doi:10.1103/PhysRevD.87.011301 [arXiv:1209.1489 [hep-ph]].

V. Martn Lozano, J. M. Moreno and C. B. Park, "Resonant Higgs boson pair production in the $hh \to b\bar{b}\ WW \to b\bar{b}\ell^+\nu\ell^-\overline{\nu}$ decay channel," JHEP **1508**, 004 (2015) doi:10.1007/JHEP08(2015)004 [arXiv:1501.03799 [hep-ph]].

[12] M. J. Dolan, C. Englert and M. Spannowsky, "Higgs self-coupling measurements at the LHC," JHEP **1210** (2012) 112 doi:10.1007/JHEP10(2012)112 [arXiv:1206.5001 [hep-ph]].

F. Goertz, A. Papaefstathiou, L. L. Yang and J. Zurita, "Higgs Boson self-coupling measurements using ratios of cross sections," JHEP **1306** (2013) 016 doi:10.1007/JHEP06(2013)016 [arXiv:1301.3492 [hep-ph]].

M. J. Dolan, C. Englert, N. Greiner, K. Nordstrom and M. Spannowsky, "$hhjj$ production at the LHC," Eur. Phys. J. C **75** (2015) no.8, 387 doi:10.1140/epjc/s10052-015-3622-3 [arXiv:1506.08008 [hep-ph]].

A. Adhikary, S. Banerjee, R. K. Barman, B. Bhattacherjee and S. Niyogi, "Revisiting the non-resonant Higgs pair production at the HL-LHC," JHEP **07** (2018), 116 doi:10.1007/JHEP07(2018)116 [arXiv:1712.05346 [hep-ph]].

S. Banerjee, C. Englert, M. L. Mangano, M. Selvaggi and M. Spannowsky, "hh + jet production at 100 TeV," Eur. Phys. J. C **78** (2018) no.4, 322 doi:10.1140/epjc/s10052-018-5788-y [arXiv:1802.01607 [hep-ph]].

J. H. Kim, M. Kim, K. Kong, K. T. Matchev and M. Park, "Portraying Double Higgs at the Large Hadron Collider," JHEP **1909**, 047 (2019) doi:10.1007/JHEP09(2019)047 [arXiv:1904.08549 [hep-ph]].

[13] ATLAS Collaboration, "Measurement prospects of the pair production and self–couling of the HIggs boson with the ATLAS experiment at the HL–LHC", ATL-PHYS-PUB-2018-053.

[14] C. O. Dib, R. Rosenfeld and A. Zerwekh, "Double Higgs production and quadratic divergence cancellation in little Higgs models with T parity," JHEP **0605**, 074 (2006) doi:10.1088/1126-6708/2006/05/074 [hep-ph/0509179].

A. Arhrib, R. Benbrik, C. H. Chen, R. Guedes and R. Santos, "Double Neutral Higgs production in the Two-Higgs doublet model at the LHC," JHEP **0908**, 035 (2009) doi:10.1088/1126-6708/2009/08/035 [arXiv:0906.0387 [hep-ph]].

R. Grober and M. Muhlleitner, "Composite Higgs Boson Pair Production at the LHC," JHEP **1106**, 020 (2011) doi:10.1007/JHEP06(2011)020 [arXiv:1012.1562 [hep-ph]].

M. Gillioz, R. Grober, C. Grojean, M. Muhlleitner and E. Salvioni, "Higgs Low-Energy Theorem (and its corrections) in Composite Models," JHEP **1210**, 004 (2012) doi:10.1007/JHEP10(2012)004 [arXiv:1206.7120 [hep-ph]].

C. Han, X. Ji, L. Wu, P. Wu and J. M. Yang, "Higgs pair production with SUSY QCD correction: revisited under current experimental constraints," JHEP **1404**, 003 (2014) doi:10.1007/JHEP04(2014)003 [arXiv:1307.3790 [hep-ph]].

K. Nishiwaki, S. Niyogi and A. Shivaji, "ttH Anomalous Coupling in Double Higgs Production," JHEP **1404**, 011 (2014) doi:10.1007/JHEP04(2014)011 [arXiv:1309.6907 [hep-ph]].

J. M. No and M. Ramsey-Musolf, "Probing the Higgs Portal at the LHC Through Resonant di-Higgs Production," Phys. Rev. D **89**, no. 9, 095031 (2014) doi:10.1103/PhysRevD.89.095031 [arXiv:1310.6035 [hep-ph]].

C. R. Chen and I. Low, "Double take on new physics in double Higgs boson production," Phys. Rev. D **90**, no. 1, 013018 (2014) doi:10.1103/PhysRevD.90.013018 [arXiv:1405.7040 [hep-ph]].

B. Hespel, D. Lopez-Val and E. Vryonidou, "Higgs pair production via gluon fusion in the Two-Higgs-Doublet Model," JHEP **1409**, 124 (2014) doi:10.1007/JHEP09(2014)124 [arXiv:1407.0281 [hep-ph]].

B. Bhattacherjee and A. Choudhury, "Role of supersymmetric heavy Higgs boson production in the self-coupling measurement of 125 GeV Higgs boson at the LHC," Phys. Rev. D **91**, 073015 (2015) doi:10.1103/PhysRevD.91.073015 [arXiv:1407.6866 [hep-ph]].

V. Barger, L. L. Everett, C. B. Jackson, A. D. Peterson and G. Shaughnessy, "New physics in resonant production of Higgs boson pairs," Phys. Rev. Lett. **114**, no. 1, 011801 (2015) doi:10.1103/PhysRevLett.114.011801 [arXiv:1408.0003 [hep-ph]].

N. Liu, S. Hu, B. Yang and J. Han, "Impact of top-Higgs couplings on Di-Higgs production at future colliders," JHEP **1501**, 008 (2015) doi:10.1007/JHEP01(2015)008 [arXiv:1408.4191 [hep-ph]].

F. Goertz, A. Papaefstathiou, L. L. Yang and J. Zurita, "Higgs boson pair production in the D=6 extension of the SM," JHEP **1504**, 167 (2015) doi:10.1007/JHEP04(2015)167 [arXiv:1410.3471 [hep-ph]].

A. Papaefstathiou, "Discovering Higgs boson pair production through rare final states at a 100 TeV collider," Phys. Rev. D **91**, no. 11, 113016 (2015) doi:10.1103/PhysRevD.91.113016 [arXiv:1504.04621 [hep-ph]].

R. Grober, M. Muhlleitner, M. Spira and J. Streicher, "NLO QCD Corrections to Higgs Pair Production including Dimension-6 Operators," JHEP **1509**, 092 (2015) doi:10.1007/JHEP09(2015)092 [arXiv:1504.06577 [hep-ph]].

C. T. Lu, J. Chang, K. Cheung and J. S. Lee, "An exploratory study of Higgs-boson pair production," JHEP **1508**, 133 (2015) doi:10.1007/JHEP08(2015)133 [arXiv:1505.00957 [hep-ph]].

S. M. Etesami and M. Mohammadi Najafabadi, "Double Higgs boson production with a jet substructure analysis to probe extra dimensions," Phys. Rev. D **92**, no. 7, 073013 (2015) doi:10.1103/PhysRevD.92.073013 [arXiv:1505.01028 [hep-ph]].

H. J. He, J. Ren and W. Yao, "Probing new physics of cubic Higgs boson interaction via Higgs pair production at hadron colliders," Phys. Rev. D **93**, no. 1, 015003 (2016) doi:10.1103/PhysRevD.93.015003 [arXiv:1506.03302 [hep-ph]].

Q. H. Cao, B. Yan, D. M. Zhang and H. Zhang, "Resolving the Degeneracy in Single Higgs Production with Higgs Pair Production," Phys. Lett. B **752**, 285 (2016) doi:10.1016/j.physletb.2015.11.045 [arXiv:1508.06512 [hep-ph]].

Q. H. Cao, G. Li, B. Yan, D. M. Zhang and H. Zhang, "Double Higgs production at the 14 TeV LHC and a 100 TeV *pp* collider," Phys. Rev. D **96**, no. 9, 095031 (2017) doi:10.1103/PhysRevD.96.095031 [arXiv:1611.09336 [hep-ph]].

T. Corbett, A. Joglekar, H. L. Li and J. H. Yu, "Exploring Extended Scalar Sectors with Di-Higgs Signals: A Higgs EFT Perspective," JHEP **1805**, 061 (2018) doi:10.1007/JHEP05(2018)061 [arXiv:1705.02551 [hep-ph]].

[15] G. Aad *et al.* [ATLAS Collaboration], "Combination of searches for Higgs boson pairs in *pp* collisions at $\sqrt{s}$ =13 TeV with the ATLAS detector," Phys. Lett. B **800**, 135103 (2020) doi:10.1016/j.physletb.2019.135103 [arXiv:1906.02025 [hep-ex]].

[16] A. M. Sirunyan *et al.* [CMS Collaboration], "Combination of searches for Higgs boson pair production in proton-proton collisions at $\sqrt{s} = 13$ TeV," Phys. Rev. Lett. **122**, no. 12, 121803 (2019) doi:10.1103/PhysRevLett.122.121803 [arXiv:1811.09689 [hep-ex]].

[17] M. Cepeda *et al.*, "Report from Working Group 2 : Higgs Physics at the HL-LHC and HE-LHC," CERN Yellow Rep. Monogr. **7**, 221 (2019) doi:10.23731/CYRM-2019-007.221 [arXiv:1902.00134 [hep-ph]].

[18] K. Fujii *et al.*, "Physics Case for the International Linear Collider," arXiv:1506.05992 [hep-ex].

[19] J. Braathen and S. Kanemura, "Leading two-loop corrections to the Higgs boson self-couplings in models with extended scalar sectors," arXiv:1911.11507 [hep-ph].

[20] J. Chang, K. Cheung, J. S. Lee, C. T. Lu and J. Park, "Higgs-boson-pair production $H(\to b\bar{b})H(\to \gamma\gamma)$ from gluon fusion at the HL-LHC and HL-100 TeV hadron collider," Phys. Rev. D **100**, no. 9, 096001 (2019) doi:10.1103/PhysRevD.100.096001 [arXiv:1804.07130 [hep-ph]].

[21] J. Chang, K. Cheung, J. S. Lee and J. Park, "Probing the trilinear Higgs boson self-coupling at the high-luminosity LHC via multivariate analysis," Phys. Rev. D **101**, no. 1, 016004 (2020) doi:10.1103/PhysRevD.101.016004 [arXiv:1908.00753 [hep-ph]].

[22] G. Heinrich, S. P. Jones, M. Kerner, G. Luisoni and E. Vryonidou, "NLO predictions for Higgs boson pair production with full top quark mass dependence matched to parton showers," JHEP **1708** (2017) 088 doi:10.1007/JHEP08(2017)088 [arXiv:1703.09252 [hep-ph]].

[23] G. Heinrich, S. P. Jones, M. Kerner, G. Luisoni and L. Scyboz, "Probing the trilinear Higgs boson coupling in di-Higgs production at NLO QCD including parton shower effects," JHEP **1906** (2019) 066 doi:10.1007/JHEP06(2019)066 [arXiv:1903.08137 [hep-ph]].

[24] M. Grazzini, G. Heinrich, S. Jones, S. Kallweit, M. Kerner, J. M. Lindert and J. Mazzitelli, "Higgs boson pair production at NNLO with top quark mass effects," JHEP **1805** (2018) 059 doi:10.1007/JHEP05(2018)059 [arXiv:1803.02463 [hep-ph]].

[25] L. B. Chen, H. T. Li, H. S. Shao and J. Wang, "Higgs boson pair production via gluon fusion at N^{3}LO in QCD," Phys. Lett. B **803** (2020), 135292 doi:10.1016/j.physletb.2020.135292 [arXiv:1909.06808 [hep-ph]].

L. B. Chen, H. T. Li, H. S. Shao and J. Wang, "The gluon-fusion production of Higgs boson pair: N^{3}LO QCD corrections and top-quark mass effects," JHEP **03** (2020), 072 doi:10.1007/JHEP03(2020)072 [arXiv:1912.13001 [hep-ph]].

[26] P. Artoisenet, R. Frederix, O. Mattelaer and R. Rietkerk, "Automatic spin-entangled decays of heavy resonances in Monte Carlo simulations," JHEP **1303**, 015 (2013) doi:10.1007/JHEP03(2013)015 [arXiv:1212.3460 [hep-ph]].

[27] R. Contino, D. Curtin, A. Katz, M. Mangano, G. Panico, M. Ramsey-Musolf, G. Zanderighi *et al.*, "Physics at a 100 TeV pp collider: Higgs and EW symmetry breaking studies," CERN Yellow Rep. (2017) no.3, 255-440 doi:10.23731/CYRM-2017-003.255 [arXiv:1606.09408 [hep-ph]].

[28] S. Dulat *et al.*, "New parton distribution functions from a global analysis of quantum chromodynamics," Phys. Rev. D **93** (2016) no.3, 033006 doi:10.1103/PhysRevD.93.033006 [arXiv:1506.07443 [hep-ph]].

[29] M. L. Mangano, M. Moretti, F. Piccinini and M. Treccani, "Matching matrix elements and shower evolution for top-quark production in hadronic collisions," JHEP **0701** (2007) 013 doi:10.1088/1126-6708/2007/01/013 [hep-ph/0611129].

[30] J. Alwall *et al.*, "Comparative study of various algorithms for the merging of parton showers and matrix elements in hadronic Eur. Phys. J. C **53** (2008) 473 doi:10.1140/epjc/s10052-007-0490-5 [arXiv:0706.2569 [hep-ph]].

[31] T. Sjstrand *et al.*, "An Introduction to PYTHIA 8.2," Comput. Phys. Commun. **191**, 159 (2015) doi:10.1016/j.cpc.2015.01.024 [arXiv:1410.3012 [hep-ph]].

[32] J. de Favereau *et al.* [DELPHES 3 Collaboration], "DELPHES 3, A modular framework for fast simulation of a generic collider experiment," JHEP **1402**, 057 (2014) doi:10.1007/JHEP02(2014)057 [arXiv:1307.6346 [hep-ex]].

[33] J. Alwall, R. Frederix, S. Frixione, V. Hirschi, F. Maltoni, O. Mattelaer, H. S. Shao, T. Stelzer, P. Torrielli and M. Zaro, "The automated computation of tree-level and next-to-leading order differential cross sections, and their matching to parton shower simulations," JHEP **07** (2014), 079 doi:10.1007/JHEP07(2014)079 [arXiv:1405.0301 [hep-ph]].

[34] A. Hoecker, P. Speckmayer, J. Stelzer, J. Therhaag, E. von Toerne, and H. Voss, "TMVA: Toolkit for Multivariate Data Analysis," PoS A CAT 040 (2007) [physics/0703039].

[35] Rene Brun and Fons Rademakers, ROOT - An Object Oriented Data Analysis Framework, Proceedings AIHENP'96 Workshop, Lausanne, Sep. 1996, Nucl. Inst. & Meth. in Phys. Res. A 389 (1997) 81-86. See also root.cern.ch/.

[36] G. Cowan, K. Cranmer, E. Gross and O. Vitells, "Asymptotic formulae for likelihood-based tests of new physics," Eur. Phys. J. C **71** (2011), 1554 doi:10.1140/epjc/s10052-011-1554-0 [arXiv:1007.1727 [physics.data-an]].

[37] M. L. Mangano, G. Ortona and M. Selvaggi, "Measuring the Higgs self-coupling via Higgs-pair production at a 100 TeV p-p collider," [arXiv:2004.03505 [hep-ph]].